

Augmented Digital Twin for Identification of Most Critical Cyberattacks in Industrial Systems

Bruno P. Leao, Jagannadh Vempati, Siddharth Bhela, *Member, IEEE*, Tobias Ahlgrim, and Daniel Arnold, *Member, IEEE*

Abstract—This work presents a novel methodology for identification of the most critical cyberattacks that may disrupt the operation of an industrial system. Application of the proposed framework can enable the design and development of advanced cybersecurity functionality for a wide range of industrial applications. The attacks are assessed taking into direct consideration how they impact the system operation as measured by a defined Key Performance Indicator (KPI). A simulation, or Digital Twin (DT), of the industrial process is employed for calculation of the KPI based on operating conditions. Such DT is augmented with a layer of information describing the computer network topology, connected devices, and potential actions an adversary can take associated to each device or network link. Each possible action is associated with an abstract measure of effort, which is interpreted as a cost. It is assumed that the adversary has a corresponding budget that constrains the selection of the sequence of actions defining the progression of the attack. A dynamical system comprising a set of states associated to the cyberattack (cyber states) and transition logic for updating their values is also proposed. The resulting Augmented Digital Twin (ADT) is then employed in a sequential decision-making optimization formulated to yield the most critical attack scenarios as measured by the defined KPI. The methodology is successfully tested based on an electrical power distribution system simulation.

Index Terms—Artificial Intelligence, Cyberattack, Digital Twins, Optimization, Threat Modeling

I. INTRODUCTION

The design and implementation of advanced cybersecurity solutions is a very challenging task due to a number of reasons. The variety of possible cyberattack scenarios to consider can be enormous and they change over time as new vulnerabilities are identified and new hardware and software are integrated into systems. The availability of historical data associated to cyberattacks is also very limited, as they are in general rare events and corresponding data, when collected, is usually

confidential in nature. Cybersecurity of industrial systems pose relevant additional challenges as each such system has in general very unique characteristics such as unique hardware, software or operating condition. They are also many times subject to increased exposure to vulnerabilities compared to information technology (IT) systems due to factors such as adoption of legacy communication protocols and challenges in patching as such procedures usually require down time. Despite such challenges, the need for advanced cybersecurity solutions for industrial systems is increasing faster than ever before as Industry 4.0 trends materialize, especially the Industrial Internet of Things (IIoT) which expands the set of possible targets for adversaries [1].

This work presents a novel solution that enables proper testing and validation of advanced cybersecurity functionality for industrial systems, with special focus on cases where the goal of the adversary is the disruption of system operation. Those are critical situations as they may have relevant negative financial and safety-related consequences. The proposed solution aims at identifying the most critical attack paths an adversary can take to disrupt specific key performance indicators (KPIs) of the industrial process. This information can then be employed to generate key test points for design and validation of advanced cybersecurity solutions.

Previous works in literature focusing on detection and mitigation of cyber threats affecting the operation of industrial processes usually fall in one of two categories: (1) considering only the consequences of the attack in system operation by monitoring the associated physical quantities and disregarding the aspects related to network communication [2]; (2) focusing on the computer network perspective and taking the system operation into account only indirectly, for instance, by defining abstractions such as critical assets which must be protected [3]. The latter is also the perspective taken by well established cybersecurity practices and tools, which in general have been adapted from an IT domain to work on Operational Technology (OT) applications.

The solution described here integrates both aspects of system operation and network communication, providing a valuable analysis of possible threats. System operation is included by means of a simulation model or digital twin (DT) of the system. The DT is employed to translate any operating conditions, including cyberattack situations, into their corresponding operational KPIs. Such system DT is augmented by a layer of information about the computer network and its cybersecurity characteristics, hereafter referred

Manuscript submitted 7 June 2023. This work was supported by the Cybersecurity, Energy Security, and Emergency Response (CESER), Risk Management Tools and Technologies (RMT) Program of the U.S. Department of Energy via the Supervisory Parameter Adjustment for Distribution Energy Storage (SPADES) Project under Contract DE-AC02-05CH11231. (Corresponding author: Bruno P. Leao.)

Bruno P. Leao, Jagannadh Vempati, Siddharth Bhela and Tobias Ahlgrim are with Siemens Technology, Princeton, NJ 08540 USA (e-mail: bruno.leao@siemens.com; jagannadh.vempati@siemens.com; siddharth.bhela@siemens.com; tobias.ahlgrim@siemens.com).

Daniel Arnold is with the Lawrence Berkeley National Lab, Berkeley, CA 94720 USA (e-mail: dbarnold@lbl.gov).

to as cybersecurity information layer (CIL). By means of this augmentation, the relevant cyber-related aspects associated to the computation devices and communication links can be properly taken into consideration in the analysis of the physical system without the burden, complexity and computational costs associated with an emulation of the computation devices and network. Finally, a sequential decision-making optimization (SDMO) framework based on Monte Carlo Tree Search (MCTS) methods is employed to interact with the DT and CIL in order to identify the attack paths which cause the greatest damage to system operation. The diagram in figure 1 depicts the three main components of the solution and their interrelation.

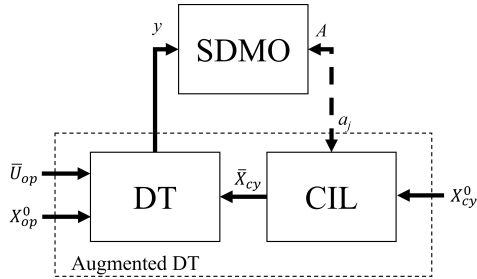


Fig. 1. High-level structure of the proposed solution with three main components: Digital Twin of the industrial system (DT), cybersecurity information layer (CIL) and sequential decision-making optimization (SDMO). DT and CIL combined form the Augmented DT (ADT). Solid arrows indicate information exchanged once for each evaluated attack scenario while the dashed arrow indicates information exchanged multiple times for each evaluated attack scenario. Details about the symbols presented in the figure are described in section II-A.

By employing the proposed solution, designers of advanced cybersecurity tools can directly take into consideration any set of relevant system operation KPIs, obtaining the most critical attack paths for properly testing the tool under development. Such attack paths are defined in a realistic setting that includes the dynamics and constraints of real world adversary actions.

A. Previous Work

The proposed methodology can be compared to previous works in literature related to cybersecurity risk assessment and quantification and their application to industrial systems. Several risk assessment methods documented in the literature incorporate probabilistic analysis using Markov chains and Bayesian networks [4]. Zhang et al. [5] explore four attack scenarios in SCADA networks, utilizing Bayesian attack graph models to assess the probabilities of successful cyber attacks. In this work, the authors utilize mean-time-to-compromise (MTTC) model to estimate the time intervals for successfully intruding cyber components in control networks. Simulation results indicate that the system's reliability decreases as the frequency and sophistication of successful cyber attacks on the SCADA components increase.

Several techniques in this field also leverage attack graphs [5]–[9]. This graphical representation models the potential paths an adversary could take to compromise a system or network. Attack graphs identify the relationships between different vulnerabilities and attack vectors that an adversary could potentially exploit to gain unauthorized access to a target

system. This approach is highly effective in generating potential attack paths and has been widely used in evaluating the security of various systems, including cyber-physical infrastructure such as the electric grid. The attack graph methodology allows for the identification and prioritization of critical assets and can aid in improving the overall security posture of the system. The graph can be constructed using automated tools such as MulVAL [10]–[12] that map network topology, system configuration, and known vulnerabilities.

Patapanchala PS et al. [13] propose a novel way to identify and prioritize critical assets and help operators take steps to improve the overall security posture of the system. In their work, they explore security metrics that can be used to monitor the cybersecurity posture of the cyber-physical system (CPS) and the physical impact of an attack while considering individual and coordinated actions that can cause cascading outages. The authors demonstrate their metrics using cyber-physical models for 9-bus and 39-bus test systems.

Kriaa et al. [14] conducted a comprehensive survey of existing approaches to industrial facility design and risk assessment that consider safety and security. They focused on the convergence of safety and security concerns in the context of the migration towards digital control systems, which creates new security threats that can endanger the safety of industrial infrastructures. The authors also conducted a comparative analysis of the different approaches identified in the literature. However, there are yet to be established approaches for evaluating the influence of cybersecurity risks on higher-level processes and their corresponding organizational impact.

In [8] a new method is proposed for assessing the impact of an attack on a business process-support enterprise network and generating a numerical score for the impact. The approach involves constructing a connected graph that maps out the dependencies between vulnerabilities on hosts, the relationships between services and hosts, and the dependencies between tasks and services. The authors leverage MulVAL to generate the graph by encoding the dependencies with Datalog [15], which is a declarative logic programming language. Finally, they calculate the impact score based on the Common Vulnerability Scoring System (CVSS) ¹ scores of the vulnerabilities by propagating the information through the interconnected graph. CVSS is a widely used framework for assessing the severity of security vulnerabilities.

In their research, Haque et al. [9] propose a graphical modeling technique that integrates mission-centric impact assessment of cyber attacks with a focus on operational resiliency. Their proposed approach combines the logical attack graph and mission impact propagation graph to calculate the impact of cyber attacks on the operational mission. Considering budgetary restrictions, an optimization process is also provided to minimize this effect. The authors demonstrate their modeling techniques through a case study involving SCADA systems for cyber-physical power systems. They suggest that by evaluating and minimizing the impact of cyber attacks on the operation of cyber-physical systems (CPS), their proposed method can

¹<https://www.first.org/cvss/>

enhance cyber resiliency.

The work proposed by Semertzis *et al.* [16] closely aligns with our proposed research. This work introduces a quantitative risk assessment method for cyber-physical systems, employing probabilistic and deterministic techniques. The method utilizes attack graphs to assess the likelihood of attacks and a dynamic cyber-physical power system model (DT) to simulate the impact of cyber attacks on power system cascading failures. A domain-specific language is proposed to describe digital substation assets and model attack graphs. The method calculates combined risk metrics considering the likelihood and impact of cyber threat scenarios. The risk assessment is performed on the IEEE 39-bus system, revealing that targeted cyber attacks on specific substations can result in significant cascading failures or even a blackout.

The risk assessment methods mentioned above are mostly qualitative in nature or focus on employing probabilistic models to analyze the impact on a single layer of CPS. They often rely on small-scale networks and primarily focus on computer network perspectives, indirectly considering system operation through abstractions like critical assets. In contrast, our work focuses on quantitative risk assessment, pinpointing the most critical cyberattacks that can potentially disrupt industrial system operations. We directly assess these attacks by evaluating their impact based on system operational KPIs. Our solution stands out by integrating system operation and network communication resulting in a comprehensive analysis of potential threats. It is also agnostic to any specific OT operations and applies to a wide range of industrial systems. Based on the critical attack paths derived from our solution, organizations can adequately prioritize their defense strategy and develop advanced cyber-defense capabilities.

B. Major Contributions

The major contributions of this work are:

- A novel methodology that provides means for assessing the most critical cyberattacks aimed at disrupting operation of industrial system as measured by defined operational KPIs.
- The means for integrating industrial system DTs into the analysis and augmenting them with the information required for implementation of the methodology.
- Empirical testing of the methodology with a realistic use case focused on a power distribution grid.

The remainder of the paper is organized as follows: section II contains all aspects of the methodology including the definitions associated to the Augmented DT (ADT), both in terms of the additional information required and how it is processed, as well as the optimization problem formulation and proposed solution; in section III the experiments and corresponding results are presented and discussed; section IV corresponds to conclusion and future work.

II. METHODOLOGY

A. Augmented Digital Twin (ADT)

The starting point of the methodology is a DT of the industrial system under analysis. Equation 4 describes the

main operation performed by the DT. Ω^σ corresponds to the information defining a cyberattack scenario. y represents the KPI value of interest quantifying how well the system operates during such scenario. y is a scalar variable which can be produced through a combination, e.g. weighted sum, of multiple other KPIs. The higher the value of y the better the system is operating, therefore the goal of an adversary who wants to disrupt the system operation could be the minimization of y or equivalently the maximization of y' as defined in the equation. Section II-B presents a definition of the optimization problem.

The DT comprises functionality for simulating the industrial system of interest. In order to take into consideration the relevant information about network communication and cybersecurity, the DT is augmented by the CIL, resulting in the Augmented DT (ADT) as presented in figure 1. CIL provides information about a cyberattack on the form of a state vector containing what is hereafter referred to as cyber states. Besides simulation of the industrial system, the DT also implements function $g_{DT}(\cdot)$ (equation 4) used for calculating the KPI value y^σ which is the outcome of attack scenario σ . Cyberattack scenario information Ω^σ (equation 1) is a set that includes two sequences which combined with initial conditions for the system simulation (X_{op}^0) and cyber states (X_{cy}^0) provide all the information required for simulating the system of interest considering cyberattack scenario σ :

- \bar{U}_{op}^σ : a sequence of inputs defining the normal operating conditions of the system (equation 2).
- \bar{X}_{cy}^σ : a sequence of cyber states defining the progression of an attack (equation 3). Only a subset of the cyber states is relevant for the DT, consisting of those related to the adversary actions which have an impact in the industrial system of interest. They correspond to actions of category *end effect* as explained in section II-A.4

The DT is employed as a black-box in the optimization process which makes the solution agnostic to the application domain and implementation details or characteristics of the DT.

$$\Omega^\sigma = \{\bar{U}_{op}^\sigma, \bar{X}_{cy}^\sigma, X_{op}^0, X_{cy}^0\} \quad (1)$$

$$\bar{U}_{op}^\sigma = [U_{op,1}^\sigma, U_{op,2}^\sigma, \dots, U_{op,z_{op}}^\sigma] \quad (2)$$

$$\bar{X}_{cy}^\sigma = [X_{cy,1}^\sigma, X_{cy,2}^\sigma, \dots, X_{cy,z_{cy}}^\sigma] \quad (3)$$

$$y^\sigma = g_{DT}(\Omega^\sigma) \quad (4)$$

The CIL comprises two parts:

- 1) a collection of information about each device and network link in the system, hereafter referred to as cybersecurity information (CI). This is specific to the industrial application under consideration.
- 2) an engine for sequentially updating cyber states given adversary actions (a_j), providing the sequence of cyber states defining an attack scenario (\bar{X}_{cy}), and identifying all possible actions the adversary can take (A) given a certain cyber state. This engine is hereafter referred to as cybersecurity information engine (CIE) and it is application agnostic.

1) *CI*: The CI comprises a set of specifications for each device and for each network link. Equation 5 describes CI as a set with two subsets, S^d and S^l , corresponding respectively to specifications of devices and specifications of network links.

$$CI = \{S^d, S^l\} \quad (5)$$

Equations 6 to 10 describe the specifications associated to devices as indicated by the d superscript. In such equations, s^{d_i} corresponds to the specifications for the i^{th} device, n^d being the total number of devices. Specifications for device i correspond to its type $\tau^{d_i} \in T$ and the set of all actions an adversary can take when interacting with it (α^{d_i}). There is a total of m^{d_i} possible actions for an adversary to interact with d_i , although many of those actions may not be accessible under many circumstances as explained in section II-A.3. Each possible

action $a_j^{d_i}$ consists of a set that includes an action type $\psi_j^{d_i} \in \Psi(\tau^{d_i})$, a set of parameters $\theta_j^{d_i}$ which are a function of the action type, and a cost $\phi_j^{d_i}$ which quantifies the effort required for executing the corresponding action. The set of parameters $\theta_j^{d_i}$ includes a category $\gamma_j^{d_i}$ which can be one of *exposure*, *exploitability* or *end effect*. Those categories, explained in detail in section II-A.4, define what other parameters are included. $e_j^{d_i}$ is an indicator function which is 1 if the action of category *exposure* corresponds to an entry point and 0 otherwise. $\zeta_j^{d_i}$ and $\xi_j^{d_i}$ are respectively a set of *end effect* attacks which become available and a set of other devices which become visible following execution of an action of category *exploitability*. Finally, $\pi_j^{d_i}$ corresponds to the mapping to a function which is part of the DT and implements the effect in simulation associated to an action of category *end effect*.

$$S^d = \{s^{d_1}, s^{d_2}, \dots, s^{d_{n^d}}\} \quad (6)$$

$$s^{d_i} = \{\tau^{d_i}, \alpha^{d_i}\}, i = 1, 2, \dots, n^d, \tau^{d_i} \in T \quad (7)$$

$$\alpha^{d_i} = \{a_1^{d_i}, a_2^{d_i}, \dots, a_{m^{d_i}}^{d_i}\} \quad (8)$$

$$a_j^{d_i} = \{\psi_j^{d_i}, \theta_j^{d_i}(\psi_j^{d_i}), \phi_j^{d_i}\}, \psi_j^{d_i} \in \Psi(\tau^{d_i}), \phi_j^{d_i} \in \mathbb{R}_+, j = 1, \dots, m^{d_i} \quad (9)$$

$$\theta_j^{d_i} = \begin{cases} \{\gamma_j^{d_i}, e_j^{d_i}\} & \text{if } \gamma_j^{d_i} = \text{exposure} \\ \{\gamma_j^{d_i}, \zeta_j^{d_i}, \xi_j^{d_i}\} & \text{if } \gamma_j^{d_i} = \text{exploitability}, \gamma_j^{d_i} \in \{\text{exposure}, \text{exploitability}, \text{end effect}\} \\ \{\gamma_j^{d_i}, \pi_j^{d_i}\} & \text{if } \gamma_j^{d_i} = \text{end effect} \end{cases} \quad (10)$$

$$S^l = \{s^{l_1}, s^{l_2}, \dots, s^{l_{n^l}}\} \quad (11)$$

$$s^{l_i} = \{\delta^{l_i}, \alpha^{l_i}, L^{l_i}\}, i = 1, 2, \dots, n^l \quad (12)$$

$$\delta^{l_i} = \{d_{f^{l_i}}, d_{t^{l_i}}\} \quad (13)$$

$$\alpha^{l_i} = \{a_1^{l_i}, a_2^{l_i}, \dots, a_{m^{l_i}}^{l_i}\} \quad (14)$$

$$L^{l_i} = \{\lambda_1^{l_i}, \lambda_2^{l_i}, \dots, \lambda_{o^{l_i}}^{l_i}\} \quad (15)$$

$$\lambda_k^{l_i} = \{d_{f_j^{l_i}}, d_{t_j^{l_i}}\}, k = 1, \dots, o^{l_i} \quad (16)$$

$$a_j^{l_i} = \{\psi_j^{l_i}, \theta_j^{l_i}(\psi_j^{l_i}), \phi_j^{l_i}\}, \psi_j^{l_i} \in \Psi(L^{l_i}), \phi_j^{l_i} \in \mathbb{R}_+, j = 1, \dots, m^{l_i} \quad (17)$$

$$\theta_j^{l_i} = \begin{cases} \{\gamma_j^{l_i}, 1\} & \text{if } \gamma_j^{l_i} = \text{exposure} \\ \{\gamma_j^{l_i}, \lambda_k^{l_i}, \pi_j^{l_i}\}, \lambda_k^{l_i} \in L^{l_i} & \text{if } \gamma_j^{l_i} = \text{end effect} \end{cases}, \gamma_j^{l_i} \in \{\text{exposure}, \text{end effect}\} \quad (18)$$

Equations 11 to 18 describe the specifications associated to network links as identified by the l superscript. s^{l_i} , α^{l_i} and $a_j^{l_i}$ are network link specification, list of possible actions and individual actions in analogy to device specifications. The same analogy applies to the number of network links (n^l) and possible actions (m^{l_i}). However, there are many relevant differences between the specification of a network link and a device. s^{l_i} consists of a set containing a pair of devices δ^{l_i} and a set of logical links L^{l_i} besides α^{l_i} . The pair δ^{l_i} corresponds to the devices which are physically connected by the link. A logical link $\lambda_k^{l_i}$ represents a logical connection between a pair of devices. This concept is explained in detail in section II-A.2.

There are o^{l_i} logical links associated to l_i . The specification of possible actions is also analogous to that of devices, as it also consists of a type ($\psi_j^{l_i}$), a list of parameters which are a function of this type ($\theta_j^{l_i}$) and a cost ($\phi_j^{l_i}$). However, the set of types associated to a network link is a function of the list of logical links ($\Psi(L^{l_i})$). Differences can also be noticed in the action parameters $\theta_j^{l_i}$ as category $\gamma_j^{l_i}$ can only assume values *exposure* or *end effect*, actions of category *exposure* can only be entry points, and actions of category *end effect* are associated to a specific logical link.

It must be noticed that the possible actions of the adversary are modeled as a discrete set. Therefore, any continuous

quantity that could be manipulated as part of an attack must undergo some form of discretization before it can be integrated into the framework.

2) *Logical Links*: A logical link corresponds to a pair of devices where one produces data or information which is consumed by the other. Data or information here includes only what is relevant for the system operation. Considering for instance an industrial network where sensors and controllers are connected by means of network switches. In this case, network (physical) links are established between controllers and switches as well as sensors and switches. However, the switch is not part of any logical link as it does not produce or consume the data relevant for the system. In this case it must be noticed that one network link may be associated to multiple logical links and also a logical link may be associated to multiple network links. Figure 2 presents a more concrete example with two sensors, *A* and *B*, connected to a controller by means of a network switch. Physical (network) links connect the sensors and the controller to the switch as indicated by the solid lines in the diagram. There is no network link connecting sensors directly to the controller. Both sensors produce information which is consumed by the controller, therefore there are two logical links connecting the sensors to the controller as indicated by the dashed lines. The switch is not associated to any logical link. It can also be noticed that in this example the network link connecting the controller to the switch is associated to two logical links and each logical link is associated to two network links.

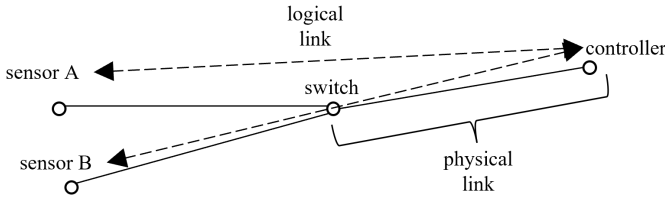


Fig. 2. Diagram representing the interconnection among devices. Solid lines indicate network (physical) links and dashed lines correspond to logical links.

3) *CIE and Augmented DT State Transitions*: Cyber states X_{cy} are a consequence of the actions performed by the adversary since the beginning of the attack and define their consequence in the industrial system as well as the awareness and access available for the adversary to take further steps. Equations 19 to 23 describe the cyber states. X_d , X_l , X_α in the equations correspond respectively to state vectors associated to devices, links and actions. There is a one-to-one association between each of those entities and a state.

$$X_{cy} = [X_d^T \ X_l^T \ X_\alpha^T]^T \quad (19)$$

$$X_d = [x_{d_1} \ x_{d_2} \ \dots \ x_{d_{n_d}}]^T \quad (20)$$

$$X_l = [x_{l_1} \ x_{l_2} \ \dots \ x_{l_{n_l}}]^T \quad (21)$$

$$X_\alpha = [x_{a_1} \ x_{a_2} \ \dots \ x_{a_M}]^T \quad (22)$$

$$M = \sum_{i=1}^{n_d} m^{d_i} + \sum_{i=1}^{n_l} m^{l_i} \quad (23)$$

TABLE I
POSSIBLE VALUES WHICH CAN BE ASSUMED BY CYBER STATES FOR EACH ENTITY TYPE

Variable	Entity Type	Possible Values
X_d	device	not visible, visible, accessible, exploited
X_l	link	not accessible, accessible
X_α	attack	not accessible, accessible, active, invalid

TABLE II
POSSIBLE STATE TRANSITIONS FOR DEVICE d^{d_i} (STATE $x_{d^{d_i}}$)

$x_{d^{d_i}}^-$	Conditions	$x_{d^{d_i}}^+$
not visible	$a_j^{d_{i'}} \mid$ $i' \neq i \wedge$ $\gamma_j^{d_{i'}} = \text{exploitability} \wedge$ $d^{d_i} \in \xi_j^{d_{i'}}$	visible
not visible	$a_j^{l_{i'}} \mid$ $\gamma_j^{l_{i'}} = \text{exposure} \wedge$ $d^{d_i} \in \delta_j^{l_{i'}}$	visible
visible	$a_j^{d_i} \mid$ $\gamma_j^{d_i} = \text{exposure}$	accessible
accessible	$a_j^{l_i} \mid$ $\gamma_j^{l_i} = \text{exploitability}$	exploited

All states are discrete and they can assume a different set of values depending on the entity type they are associated with. Table I presents this association.

State transitions happen when an adversary performs an action. Tables II to IV present all possible state transitions for each entity type. On each table, the minus (−) and plus (+) superscripts indicate respectively the state before and after the corresponding transition. All conditions listed in each row of the tables must be fulfilled in order for the corresponding transition to happen.

Section II-A.4 describes details about action categories which are useful for a better understanding of the semantics associated to the actions and the corresponding state transitions triggered by them.

The CIE is responsible for keeping track of cyber states and their transitions and extracting related information which is employed for system simulation and attack optimization. Equations 24 and 25 represent the computations performed by CIE when adversary action a_j is performed.

$$X_{cy}^+ = f_{cy}(X_{cy}^-, a_j) \quad (24)$$

TABLE III
POSSIBLE STATE TRANSITIONS FOR LINK l^{l_i} (STATE $x_{l^{l_i}}$)

$x_{l^{l_i}}^-$	Conditions	$x_{l^{l_i}}^+$
not accessible	$a_j^{d_{i'}} \mid$ $\gamma_j^{d_{i'}} = \text{exploitability} \wedge$ $d_{i'} \in \delta_j^{l_i} \wedge$ $\delta_j^{l_i} \cap \zeta_j^{d_{i'}} \neq \emptyset$	accessible
not accessible	$a_j^{l_i} \mid$ $\gamma_j^{l_i} = \text{exposure}$	accessible

TABLE IV
POSSIBLE STATE TRANSITIONS FOR ATTACK a_j (STATE x_{a_j})

$x_{a_j}^-$	Conditions	$x_{a_j}^+$
not accessible	$x_{d^{d_i}}^+ = \text{visible} \wedge$ $a_j = a_{j'}^{d_i} \wedge$ $\gamma_{j'}^{d_i} = \text{exposure}$	accessible
not accessible	$x_{d^{d_i}}^+ = \text{accessible} \wedge$ $a_j = a_{j'}^{d_i} \wedge$ $\gamma_{j'}^{d_i} = \text{exploitability}$	accessible
not accessible	$x_{l^{l_i}}^+ = \text{accessible}$ $a_j \in \alpha^{l_i}$	accessible
not accessible	$a_{j'}^{d_i} $ $\gamma_{j'}^{d_i} = \text{exploitability} \wedge$ $a_j \in \zeta_{j'}^{d_i}$	accessible
accessible	a_j	active
accessible	$x_{d^{d_i}}^+ = \text{accessible} \wedge$ $a_j = a_{j'}^{d_i} \wedge$ $\gamma_{j'}^{d_i} = \text{exposure}$	invalid

$$A^+ = g_{cy}(X_{cy}^+) \quad (25)$$

Function $f_{cy}(\cdot)$ corresponds to execution of state transitions as defined in tables II to IV based on actions taken by the adversary.

Defining S_α as the set of all attacks a_j , $j = 1, 2, \dots, M$, where the state x_{a_j} in X_{cy} refers to a_j , function $g_{cy}(\cdot)$ can then be defined as presented in equation 26.

$$g_{cy}(X_{cy}) = \{a_j \in S_\alpha | x_{a_j} = \text{accessible}\} \quad (26)$$

Both $f_{cy}(\cdot)$ and $g_{cy}(\cdot)$ are computed multiple times for each attack scenario, once for every action performed by the adversary. It is also a role of CIE to provide the sequence of cyber states defining an attack scenario (\bar{X}_{cy}) for the DT so that the KPI can be calculated according to equation 4 (figure 1). This operation ($\bar{f}_{cy}(\cdot)$) is computed once for every considered scenario. Equation 27 presents this computation for scenario σ . \bar{a}^σ corresponds to the sequence of adversary actions performed during cyberattack scenario σ .

$$\bar{X}_{cy}^\sigma = \bar{f}_{cy}(X_{cy}^0, \bar{a}^\sigma) \quad (27)$$

$$\bar{a}^\sigma = [a_1^\sigma, a_2^\sigma, \dots, a_{z_{cy}}^\sigma] \quad (28)$$

Standard initial conditions for all cyber states, as indicated by the superscript 0, are defined in equations 29 to 31 for each entity type. These definitions assume no devices or links are compromised before the beginning of the attacks, but they can be adjusted to fit other scenarios.

$$x_{d^{d_i}}^0 = \text{not visible} \quad (29)$$

$$x_{l^{l_i}}^0 = \text{not accessible} \quad (30)$$

$$x_{a_j}^0 = \begin{cases} \text{accessible,} & \text{if } \gamma_j = \text{exposure} \wedge e_j = 1 \\ \text{not accessible,} & \text{otherwise} \end{cases} \quad (31)$$

4) *Categories of Adversary Actions*: In previous sections, action categories (γ) are presented as part of CI with great relevance for aspects of the methodology such as cyber state transitions. Another fundamental concept associated to the proposed approach is that of an attack budget which is the constraint that limits the number and type of actions an adversary can take as part of an attack scenario. Those concepts and their relations are explained in detail below.

a) *Attack Budget*: In this work, we define the attack budget as quantifying the effort or resources needed or available to execute an attack scenario. The definition of such budget can have implications on the impact and likelihood of an attack scenario, including the tactics and techniques that an adversary may use. Previous works in the literature consider a budget definition for cyberattack and defense. However, such existing definitions are considered insufficient for the purpose of this work. For instance, [17] describes attack and defense budgets for investigations based in IEEE-14, 39 and 57 bus systems. In this case, each node is assumed to be a substation and the budgets are simply defined in terms of number of substations. In [18] a game-theoretical approach to attacking is described, with worst-case and random attacks utilized, but the attack and defense budgets are also defined in terms of a number of substations. Our attack budget and corresponding attack costs definitions extends these ideas to take into consideration a large variety of possible adversary actions organized in three layers: *exposure*, *exploitability*, and *end effect*.

Each action taken by the adversary in this context must be associated to a corresponding cost (ϕ as presented in previous sections). The summation of the costs associated to all attacks tried during a certain scenario must fit within the defined attack budget for that scenario. Each attack category is associated to three possible cost levels. Each action belonging to a certain category must be associated with one of the corresponding levels.

b) *Exposure*: The *exposure* category corresponds to the efforts required for accessing the target system either externally - from the internet or creating a physical security breach - or internally - by means of lateral movement. High costs for actions in this category could correspond to devices or systems that are hard to access and are well protected. Low costs on the other hand could result, for instance, from devices or systems that are directly connected to the internet with little or no protection.

Exposure costs are associated with factors such as network topology, access controls, and security posture. A subset of MITRE ATT&CK [19] tactics, techniques and procedures (TTPs) can be mapped to this category. Some examples of this mapping include:

- Network Scanning: An adversary may use network scanning to identify exposed systems or services that can be targeted for exploitation.
- Phishing: An adversary may use phishing to trick users into providing credentials or clicking on malicious links, allowing the adversary to gain access to the network.

Determining the exposure of an asset is a subjective evaluation that involves considering various factors. To compute costs

associated to actions in the *exposure* category, the following factors must be considered:

- Network Accessibility (NA): This factor represents the effort required to gain network access to the target system. It takes into account factors such as network security controls, encryption, authentication mechanisms, and network segmentation. A device directly connected to the internet and an isolated system would correspond respectively to high and low NA scores.
- Authentication Effort (AE): This factor represents the effort required to bypass or overcome authentication mechanisms to access the target system. It includes aspects such as the strength of passwords, multi-factor authentication, account lockouts, and other authentication-related defenses.
- Privilege Escalation (PE): This factor represents the effort required to elevate privileges or gain higher levels of access within the target system. It relates to aspects such as privilege separation, access controls, least privilege principles, and the complexity of privilege escalation techniques.
- Protection Level (PL): This represents the level of protection applied to the system. This may include firewall settings, antivirus software, or other cybersecurity measures.

Effort scores are associated with the abovementioned factors to determine their relative significance in the exposure assessment. These scores assigned are defined based on expert judgment by considering factors such as the potential impact of the vulnerability, likelihood of exploitation, criticality of the asset, and the system's operational requirements. The higher the weight, the more influential the factor determines the associated action cost. The final cost is obtained by the sum of the factor scores as presented in equation 32:

$$\phi_{exposure} = \phi_{NA} + \phi_{AE} + \phi_{PE} + \phi_{PL} \quad (32)$$

Each factor score have a range of values from 1 to 10, indicating their relative significance in determining the overall cost.

c) Exploitability: Actions in this category correspond to technical vulnerabilities that can be exploited by the adversary. Such actions may be associated, for instance, with software vulnerabilities and misconfigurations. The corresponding costs reflect the complexity associated to gaining access to the system to be able to execute the attack. High costs associated to an action in exploitability category could correspond to a need for specialized knowledge or even the need for a new zero-day exploit. Low costs on the other hand may be associated with known exploits that are easy to use. A subset of MITRE ATT&CK TTPs can also be mapped to this category. This includes the following:

- Exploit Public-Facing Application: An adversary may exploit vulnerabilities in public-facing applications, such as web applications or email clients, to gain access to the network.
- Remote Command Execution: This technique involves an adversary remotely executing commands on a targeted industrial control system. By exploiting vulnerabilities or

leveraging authorized remote access, the adversary gains control over the system and executes malicious commands to manipulate or disrupt its operation.

- Rogue Master: Adversaries have the capability to establish a rogue master that takes advantage of control server functionalities to communicate with outstations. This rogue master can be utilized to send control messages that appear legitimate to other control system devices, resulting in unintended impacts on processes.

To compute the costs for tasks in the exploitability category, we look to the Common Vulnerability Scoring System (CVSS)², a standardized framework for assessing the severity and impact of security vulnerabilities. The Base metric group represents the inherent qualities of a vulnerability that remain consistent regardless of time or user environments. This group comprises two sets of metrics: (i) the Exploitability metrics and (ii) the Impact metrics. The Exploitability metrics capture the ease and technical methods involved in exploiting a vulnerability. These metrics signify the attributes of the vulnerable component itself, formally known as the vulnerable entity. Exploitability metrics comprise four components – Attack Vector, Attack Complexity, Privileges Required, and User Interaction. These metrics align with our needs for calculating the attack budget. The attack budget is defined as follows:

$$\phi_{exploitability} = 100 \cdot e^{4-ES} \quad (33)$$

Equation 33 presents the calculation of costs for exploitability actions ($\phi_{exploitability}$), where ES is exploitability score from CVSS which ranges from 0.1 to 4. This is the cost to launch a significant attack, considering resources like time, personnel, and technology, without any specific vulnerability in mind. Equation 33 stands valid for CVSS version 3.1 and later.

d) End Effect: This category comprises adversary actions which directly impact the target industrial system. It includes actions that may affect the DT simulation and in turn may impact the KPI of interest (y). Some examples of how the MITRE ATT&CK TTPs can be mapped to this layer include:

- Impact to Availability: An adversary may launch a denial of service attack or destroy critical data, disrupting services and causing downtime.
- Impact to Integrity: An adversary may modify data or inject malicious code, compromising the integrity of the system or network.

The definition of costs in this category will in general be domain specific, requiring analysis from domain experts.

B. Optimization Problem Formulation

The cyberattack optimization problem can be defined as obtaining the optimal sequence of attacks \bar{a}^* that minimizes the system KPI of interest (y) as presented in equation 34. Defining β as the attack budget available to the adversary, the optimization is also subject to constraint 35.

$$\bar{a}^* = \underset{\bar{a}}{\operatorname{argmin}}(y) \quad (34)$$

²<https://www.first.org/cvss/>

$$\sum_{\kappa=1}^{z_{cy}} \phi_{\kappa} \leq \beta \quad (35)$$

C. Sequential Decision-Making Optimization

A SDMO engine is employed for iteratively searching for the sequence of attacks which is optimal in terms of causing largest disruption to a the system operational KPI of interest (equation 34). As presented in figure 1 the SDMO interacts with the CIE multiple times per attack scenario informing defined adversary actions and obtaining all possibilities for the following action (equation 25) and with the system DT in order to obtain KPI values corresponding to the current attack scenario (equation 4).

One method which can be employed for obtaining solutions to the defined problem is Monte Carlo Tree Search (MCTS) [20] as it has been successfully applied in similar sequential decision-making optimization contexts in recent years, especially for games [21]. This is the method employed in the experiments described in section III.

MCTS is a best-first search algorithm where a tree is iteratively built based on random exploration of sequences of states. Each node corresponds to a point in the state space and is associated to a value. In the context of this work, each node corresponds to a cyber state X_{cy} (equation 19). Child nodes are obtained by means of state transitions, which in this case are triggered by adversary actions as defined in equation 24. The value for a certain node is updated based on the rewards associated to exploration paths that contain such node. Here, the rewards are a function of the KPI y which is calculated using the DT (equation 4). Each path from the root to a terminal node corresponds to a sequence of cyber states \bar{X}_{cy} that define an attack scenario as described in section II-A.3.

A detailed description of the MCTS method is beyond the scope of this work and can be found in various references in literature (e.g. [20]) but a brief description is provided below, including contextualization for the problem under consideration. For each MCTS iteration, a node of the current tree is chosen, usually based on the UCT (upper confidence bound applied to trees) criteria which considers the value of each node but also provides simple means for balancing exploration and exploitation. A simulation is then run starting at the selected node and applying randomly defined actions until reaching a terminal state. In the considered context, actions are chosen among the options defined by the set A after its update based on equation 25 and terminal states are achieved when the attack budget left after subtracting the costs of all previous adversary actions is not sufficient for an additional action, as indicated in constraint 35. At each iteration, a new node is added to the tree and values of each node in the path taken during simulation are updated based on the rewards obtained until reaching the terminal state. Iterations are repeated until reaching a pre-defined limit in terms of their number or computation time.

MCTS has some characteristics which make it especially suited for solving the sequential-decision making optimization defined in equation 34. It is a so-called anytime algorithm as it can produce a valid solution even if interrupted during

computations. The DT can be employed as a black-box model that provides the reward corresponding to a certain state. It also does not require the calculation of rewards for intermediate nodes during simulation. They can be calculated only for terminal nodes.

III. EXPERIMENTS AND RESULTS

The electric power system, which is undergoing a transformation due to the proliferation of renewable generation sources and IoT devices, is becoming an increasingly popular target of cyber attacks. As the devices such as rooftop solar systems, behind the meter storage (i.e., batteries), electric vehicles, and smart appliances have inherent electronic communications capabilities, the cyber attack surface of modern electric power grids has vastly expanded [22]. Therefore, power systems correspond to a very adequate domain for application of the proposed methodology.

For this purpose the PyCIGAR tool [23] was employed. PyCIGAR is a library based in Python programming language which wraps power system simulation models developed in formats such as OpenDSS and facilitates systematic testing and integration of external logic to the simulation, especially in terms of device control. The library was extended to include control and cyberattack functionality for additional devices as described in section III-A.3.

A. Power Grid Modeling, KPIs, and Attacks

1) *Power Grid Modeling*: For the experiments, the standard IEEE 123-bus feeder model [24] was modified to custom-build a 246-bus power distribution network in OpenDSS³ as described in figure 3.

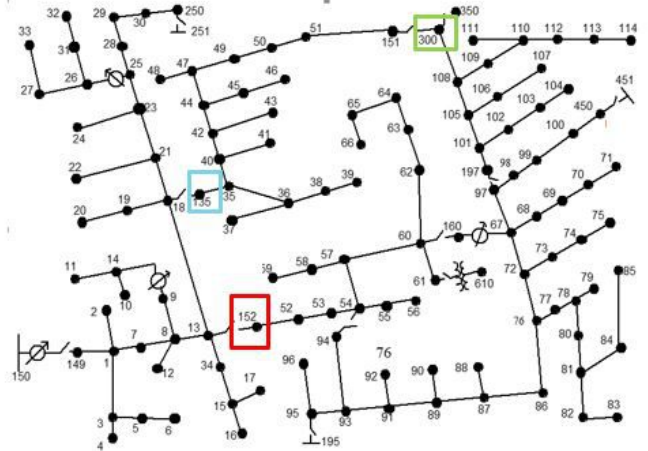


Fig. 3. Shown here is the standard IEEE 123-bus feeder model (for a single feeder) connected to the substation bus 150. The 246-bus network was built by mirroring the standard IEEE 123-bus feeder and adding it to the existing substation, i.e., the power network consisted of one substation with two 123-bus feeder models, henceforth referred to as Feeder 1 and Feeder 2. Boxes in the figure show the locations of normally open switches between the same buses (135, 152, and 300) in Feeder 1 and 2.

The 246-bus network model was augmented by normally open switches to enable topology reconfiguration operations.

³<https://www.epri.com/pages/sa/opendss>

The standard IEEE 123-bus feeder model was also modified to include additional PV (photovoltaic inverters) on every bus to represent a distribution network with high penetration of renewable energy generation. PV and load profiles consisted of a four-hour time window representing operation from 9:00 a.m. to 1:00 p.m. with a 1s sampling rate. The PV profiles were chosen to allow inter-feeder topology reconfiguration over the entire time series without overloading the substation transformer, i.e., if the topology were to be reconfigured to bring Feeder 2 onto Feeder 1, then the substation would be heavily loaded, yet it would not cause overloading or severe under voltage issues.

Three battery energy storage systems (BESS) were added to capture a realistic network with storage devices. They were randomly dispersed in the network on buses 33, 48, and 71 in Feeders 1 and 2. The control logic was set up to perform peak shaving and valley filling functions from a centralized controller that monitors the substation active power in-feed. The valley filling function enables charging when the net active power at the substation is below a specified threshold. Similarly, the peak shaving function discharges the BESS when the net active power at the substation exceeds a specified threshold. In between the thresholds for peak shaving and valley filling the BESS is neither charging nor discharging.

2) *KPIs*: Key performance indicators (KPIs) were defined to quantify how well the system is operating, which can then be used for measuring efficacy of an attack in disrupting operation (equation 4). The KPI employed for the analysis is a combination of voltage imbalance (*VI*) and substation power factor (*SPF*). We refer to this KPI as *VISPF* hereafter. The corresponding definitions are presented below.

Consider a power network comprising of N nodes modeled as a connected graph $\mathcal{G} = (\mathcal{V}, \mathcal{E})$, whose nodes $\mathcal{V} = \{1, \dots, N\}$ correspond to buses, and edges \mathcal{E} to undirected lines. Then *VI* is defined as:

$$VI = \max_{i_{ph} \in \{a_{ph}, b_{ph}, c_{ph}\}, j_{\nu} \in \mathcal{V}} \left\{ \frac{|V_{i_{ph}, j_{\nu}} - \hat{V}_{j_{\nu}}|}{\hat{V}_{j_{\nu}}} \right\} \quad (36)$$

where $V_{i_{ph}, j_{\nu}}$ are the line-to-neutral voltage magnitudes of electrical phase $i_{ph} \in \{a_{ph}, b_{ph}, c_{ph}\}$ on bus $j_{\nu} \in \mathcal{V}$ and $\hat{V}_{j_{\nu}} = \sum_{i_{ph}} V_{i_{ph}, j_{\nu}} / 3$. Similarly, *SPF* is defined as:

$$SPF = \left| \cos \left(\tanh \left(\frac{q_{ss}}{p_{ss}} \right) \right) \right| \quad (37)$$

where q_{ss} and p_{ss} are respectively the net reactive and active power at the substation obtained from summation of the values from the three phases. Lastly, the combined *VISPF* KPI is defined as:

$$VISPF = \frac{1 - VI + SPF}{2}. \quad (38)$$

The KPI values vary on a range between 0 to 1. Attacks that minimize this KPI can be considered the most effective ones (equation 34).

3) *Attack Effects in the Power System*: The PyCIGAR framework provides means to facilitate modeling of power grid devices and controllers. In the library, device models represent the interaction of specific elements with the grid, whereas controller models, as the name states, define the corresponding

control logic. Possible adversary actions were modeled as part of the controller models. This modeling results in desirable characteristics such as starting/ending actions at any point in the simulation, including multiple actions happening in parallel.

Table V presents an overview of the modeled devices and the associated possibilities in terms of adversary actions. All these actions correspond to category *end effect* as described in section II-A.4.

B. System Model Augmentation

The communication network utilized in this work was inspired by a network design developed by Cisco's Distribution Automation Feeder Automation Design Guide [25] closely emulating a Supervisory Control and Data Acquisition (SCADA) system for electrical distribution. This design served as a valuable reference point, provided insights into establishing an efficient communication framework, and allowed us to simulate real-world scenarios and evaluate the performance of our proposed methodologies within a realistic context. Various network devices, including routers, switches, and device controllers, were included associated to the power system of interest by following the SCADA architecture pattern presented in figure 4. Table VI lists the different categories of devices included in the computer network and the quantity corresponding to each type.

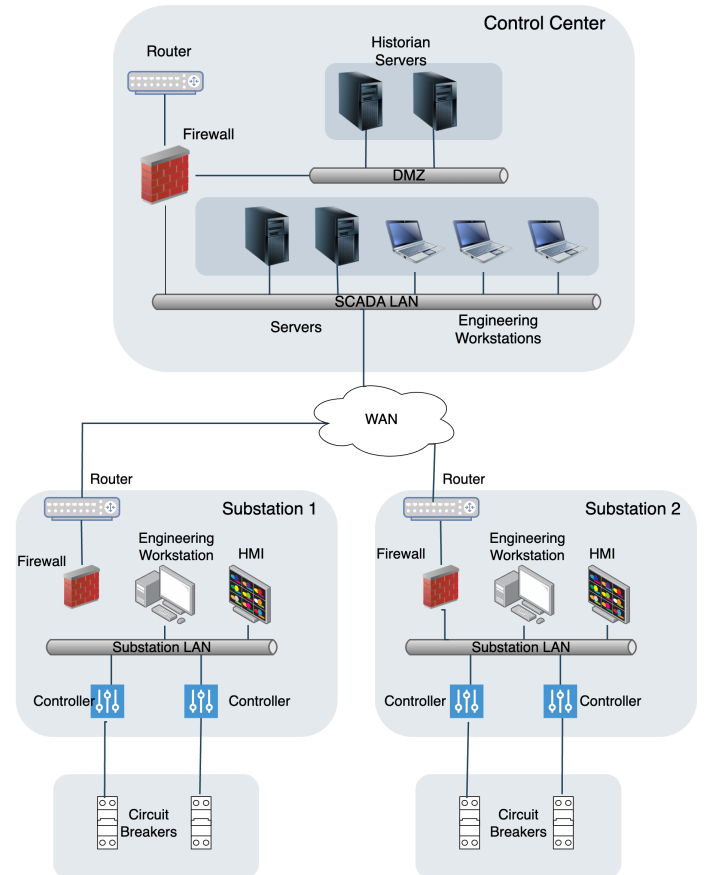


Fig. 4. SCADA system architecture pattern employed for definition of the communication network.

TABLE V
DEVICES MODELED IN PYCIGAR AND CORRESPONDING POSSIBLE ADVERSARY ACTIONS

Device	Attack	Description
PV Inverter Device	Connect/Disconnect	Disconnects the PV Device for the specified time
	VoltageBreakPoints	Modifies the Volt/Var and Volt/Watt behavior
	Unbalanced	Creates an unbalanced output across the 3 phases
Battery Storage Device	Operation Mode	Modifies the operation mode (e.g.: charge instead of discharge)
	Power Injection	Forces to discharge the battery with maximum power
	Power Consumption	Forces to charge the battery with maximum power
	Battery Settings	Modifies the control parameters (e.g.: reduce the max ramp rate)
Switch Device	Open/Close (Topology)	Operates two connected switches to change the topology
Capacitor Device	Curtailement	Reduces the capacity of the capacitor bank
Regulator Device	Change Settings	Modifies the regulator settings
	Regulator Deactivate	Fixes the regulator to a specific tap
	Regulator Prohibit Control	Prohibits the regulator from executing controls
	Change Taps	Changes the regulators tap

TABLE VI
DEVICES INCLUDED IN THE NETWORK ARCHITECTURE

Type of Device	Number of Devices
Router (Edge Device)	47
Firewall	2
Workstation	5
BESS	3
Capacitor Bank	4
Switch Controller	1
Load Controller	91
PV Inverters	91

Communication network devices and topology were then encoded using the NetJSON⁴ format. NetJSON is a data interchange format based on JavaScript Object Notation (JSON) specifically designed to describe the fundamental components of layer 2 and layer 3 networking. It was chosen as it offers a standardized and structured approach to represent network-related information, including device configurations, monitoring data, network topology, and routing information.

Details regarding potential attacker actions associated with each device and network link within different categories are also encoded in the NetJSON information, following the definitions presented in section II-A.4. For each action, the primary information recorded consists of its category and its cost. Details about the definition of costs are presented in section III-B.1

1) *Attack Costs and Budget*: Costs associated to the possible adversary actions play a crucial role in the overall analysis. Below is a description of how those values were defined for the experiments.

a) *Exposure Cost*: The exposure cost for the devices is calculated based on the four factors described in section II-A.4.b. Since these scores are subjective, they are obtained based on the evaluation by domain experts. One example describing the definition of cost for an action of category *exposure* is presented below. This action corresponds to a router which is located inside a control center.

Four factors are analyzed as described in section II-A.4: Network Accessibility (NA), Authentication Effort (AE), Privilege Escalation (PE) and Protection Level (PL). NA involves analyzing the router's configuration, topology, and

potential attack vectors. Based on these parameters and the device assessment, a 7 out of 10 score was assigned. AE represents the difficulty of bypassing or compromising the router's authentication mechanisms, an 8 out of 10 effort score was defined. PE accounts for security measures to prevent unauthorized users from accessing critical functions or data. The privilege escalation effort score in this case was 6 out of 10. For PL, as the router is situated within a control center, it is presumed that multiple layers of protection are enabled to ensure enhanced security. Hence, a score of 9 out of 10 was assigned. The total exposure cost, i.e., effort spent by the adversary to identify/detect the device, is then 30 based on the definitions above and equation 32. The exposure cost for the remaining devices is computed using a similar approach.

b) *Exploitability Cost*: The exploitability cost is calculated based on the vulnerabilities present in the device as described in section II-A.4.c. To compute the exploitability cost, as described in equation 33, we begin by identifying the vulnerabilities existing in the device. This can be accomplished by utilizing vulnerability scanning tools such as Nmap⁵, OpenVAS⁶, Tenable/Nessus⁷. Once the vulnerabilities are identified, we look up the associated Common Vulnerabilities and Exposures (CVEs) and retrieve the corresponding CVSS scores. In particular, we refer to the exploitability score of the CVEs. Considering the router from the previous scenario as an example, let's assume it has two vulnerabilities: CVE-2023-20183⁸ and CVE-2021-1619⁹. The base CVSS scores (identified from the NVD database) for these vulnerabilities are 5.4 and 9.1, and their corresponding exploitability scores are 2.8 and 3.9, respectively. From equation 33, we can compute the exploitability cost to exploit each vulnerability. Exploitability cost to exploit CVE-2023-20183 is $100 \cdot e^{(4-2.8)} = 332$ and to exploit CVE-2021-1619 is $100 \cdot e^{(4-3.9)} = 110$. We compute the exploitability cost for every device following the same approach.

For network links, besides the definition of costs for actions of category *exposure*, the mapping of all logical links

⁵<https://nmap.org/>

⁶<https://openvas.org/>

⁷<https://www.tenable.com/products/nessus>

⁸<https://nvd.nist.gov/vuln/detail/CVE-2023-20183>

⁹<https://nvd.nist.gov/vuln/detail/CVE-2021-1619>

⁴<https://netjson.org/>

corresponding to each physical link must also be performed. The functionality of the Python package NetworkX¹⁰ was employed to traverse the computer network graph defined as described above to determine such logical links. It was assumed that communication is performed between each controller and the control center. All the source nodes were first identified, and then the graph was traversed to identify the sink nodes and the paths connecting sources to sinks. The result, in the form of a list of logical links associated to each physical link, is also stored using the NetJSON format.

Concerning the costs for category *end effect*, definition was performed with support of a power systems domain expert, but the general approach consisted of considering two level of complexity: if the functionality associated with the action was already present in the device it was provided with a lower cost, while in case more complex manipulation was required, such as coding a new functionality, higher costs were defined.

C. CIE Implementation and Optimization Results

CIE logic for updating and extracting information from the cyber states as described in section II-A.3 was implemented based on the Julia programming language, using the POMDP library¹¹. This implementation included integration with the PyCIGAR-based DT for calculation of rewards. The corresponding MCTS solver¹² was employed for solution of the sequential decision making optimization as described in section II-C.

As a basis for evaluation of the quality of results, a large number of attack scenario samples were generated and evaluated for computation of the corresponding reward (4) using a node from a super computing cluster comprising an Intel Xeon Gold 5218 processor with 32 cores and 1584GB of RAM. CIE logic was enforced to constrain the attack scenarios the same way as in the analysis. All cores of the computing node were employed to generate the samples and memory sharing mechanisms were applied to minimize the repetition of samples in separate processes. A total of 504 wall-clock hours were employed for such processing, producing 504217 attack scenario samples and the corresponding reward values. An empirical cumulative distribution function (ECDF) based on the reward samples is used to evaluate the performance of the results, indicating the percentage of samples that produce rewards that are lower than the one under analysis. Such percentage will be referred to as p_{CDF} hereafter.

Optimization experiments have been performed on a computer running Ubuntu 18.04 operating system, comprising Intel Xeon Silver 4210 processor and 187GB of RAM. Table VII presents the results. All tests were performed considering the same attack budget and MCTS configurations. The durations presented in the table were normalized for a fair comparison as simulations performed later benefit from stored results produced by previous tests. It can be noticed that all results correspond to high p_{CDF} . Most results are within 0.951 and 0.984 with one exception in terms of lower value (0.931 in scenario #6)

and another corresponding to a high value (>0.999 in scenario #4). It can also be noticed from the results that increasing the number of iterations has an expected impact in duration but it does not seem to impact p_{CDF} . The possible explanation is that as all values tested for the number of iterations are the same order of magnitude and it would require order of magnitude increases in this number to obtain systematic improvements. Such order of magnitude increase would be feasible by applying some approaches described in section IV-A.

TABLE VII
OPTIMIZATION EXPERIMENTS AND RESULTS

Scenario	Iterations	Duration [h]	p_{CDF}
1	2000	27	0.984
2	2000	24	0.962
3	2000	21	>0.999
4	5000	60	0.951
5	5000	69	0.984
6	5000	60	0.931
7	7500	103	0.981
8	7500	64	0.962
9	7500	103	0.984

As an illustration of the adversary steps associated to those attack scenarios, below is a description of the steps yielded in scenario #3 which corresponds to the best p_{CDF} in table VII:

- 1) Adversary uses as entry point (*exposure* category) a network link connecting two routers which contain communication from multiple controllers but is exposed in the field and not behind a firewall. This can be considered a good trade off in terms of attack cost and impact.
- 2) Once the link is accessible, the adversary performs false data injection attacks (*end effect* category) affecting four controllers corresponding to three controllable loads and one PV inverter.

IV. CONCLUSION

This paper presented a methodology for identifying the most critical cyberattack scenarios affecting an industrial system. Criticality is assessed in terms of impact in operational performance by means of a defined KPI. Therefore, the proposed framework is focused on the operator point-of-view when evaluating what the most critical cyberattack scenarios are. The task is accomplished by employing system simulations (DTs) developed using standard engineering tools which can be augmented to include the information required for the analysis, in terms of computer network topology and devices and possible adversary actions. An attack cost-budget mechanism is employed to define adjustable constraints to the adversary actions. All the information required for augmenting the DT can be well represented using the NetJSON standard.

Once the ADT is achieved, the methodology provides means for tracking cyber states that describe the progression of attack scenarios, consisting of a sequence of adversary actions, in a way that enables the use of optimization/search methods for identification of the most critical possibilities. MCTS was proposed and successfully tested for the task, based on the model of a power distribution system. However, it must be

¹⁰<https://networkx.org/>

¹¹<https://github.com/JuliaPOMDP/POMDPs.jl>

¹²<https://github.com/JuliaPOMDP/MCTS.jl>

noted that computational cost can become prohibitive depending on the DT computational performance and the complexity of the system of interest. This is one of the main aspects which must be addressed by future work as described below.

A. Limitation and Future Work

One of the key aspects that limit the use of the proposed methodology is computational performance as it relies on the DT for calculation of KPIs which are, in turn, used as rewards for optimization/search. Considering the MCTS solution, one clear possibility to explore consists of parallelizing the calculations based on methods such as the one proposed by Liu et al. [26]. This kind of enhancement can be very desirable as it may provide benefits which are application agnostic. Heuristics can also be designed to speedup MCTS computations [20]. An alternative possibility for reducing computation costs is the use of surrogate models to replace the original DT [27], however this approach is in general very dependent on the application under consideration. It must be noted that the possibilities described above are not mutually exclusive, hence they can also be combined for additional benefit.

Another important topic for future work consists of proposing more systematic means for the definition of costs and budgets so that they are less dependent on the evaluation by subject matter experts. The incorporation of extensively adopted cybersecurity resources such as MITRE ATT&CK and CVSS in such definitions, which is already part of the methodology, is one step in this direction, however further improvements in this aspect would facilitate additional applications of the methodology.

V. ACKNOWLEDGEMENT

Any opinions, findings, conclusions, or recommendations expressed in this material are those of the authors and do not necessarily reflect those of the sponsors of this work.

REFERENCES

- [1] A. Corallo, M. Lazoi, M. Lezzi, and A. Luperto, "Cybersecurity awareness in the context of the industrial internet of things: A systematic literature review," *Computers in Industry*, vol. 137, p. 103614, 2022. [Online]. Available: <https://www.sciencedirect.com/science/article/pii/S0166361522000094>
- [2] F. Mohammadi, "Emerging challenges in smart grid cybersecurity enhancement: A review," *Energies*, vol. 14, no. 5, 2021. [Online]. Available: <https://www.mdpi.com/1996-1073/14/5/1380>
- [3] K. Le Blanc, A. Ashok, L. Franklin, J. Scholtz, E. Andersen, and M. Cassiadoro, "Characterizing cyber tools for monitoring power grid systems: What information is available and who needs it?" in *2017 IEEE International Conference on Systems, Man, and Cybernetics (SMC)*, 2017, pp. 3451–3456.
- [4] R. V. Yohanandhan, R. M. Elavarasan, P. Manoharan, and L. Mihet-Popa, "Cyber-physical power system (cpps): A review on modeling, simulation, and analysis with cyber security applications," *IEEE Access*, vol. 8, pp. 151 019–151 064, 2020.
- [5] Y. Zhang, L. Wang, Y. Xiang, and C.-W. Ten, "Power system reliability evaluation with scada cybersecurity considerations," *IEEE Transactions on Smart Grid*, vol. 6, no. 4, pp. 1707–1721, 2015.
- [6] A. T. Al Ghazo, M. Ibrahim, H. Ren, and R. Kumar, "A2g2v: Automatic attack graph generation and visualization and its applications to computer and scada networks," *IEEE Transactions on Systems, Man, and Cybernetics: Systems*, vol. 50, no. 10, pp. 3488–3498, 2020.
- [7] A. Stefanov, C.-C. Liu, M. Govindarasu, and S.-S. Wu, "Scada modeling for performance and vulnerability assessment of integrated cyber-physical systems," *International Transactions on Electrical Energy Systems*, vol. 25, no. 3, pp. 498–519, 2015.
- [8] C. Cao, L.-P. Yuan, A. Singhal, P. Liu, X. Sun, and S. Zhu, "Assessing attack impact on business processes by interconnecting attack graphs and entity dependency graphs," in *Data and Applications Security and Privacy XXXII: 32nd Annual IFIP WG 11.3 Conference, DBSec 2018, Bergamo, Italy, July 16–18, 2018, Proceedings 32*. Springer, 2018, pp. 330–348.
- [9] M. A. Haque, S. Shetty, C. A. Kamhoua, and K. Gold, "Integrating mission-centric impact assessment to operational resiliency in cyber-physical systems," in *GLOBECOM 2020 - 2020 IEEE Global Communications Conference*, 2020, pp. 1–7.
- [10] X. Ou, S. Govindavajhala, A. W. Appel et al., "Mulval: A logic-based network security analyzer." in *USENIX security symposium*, vol. 8. Baltimore, MD, 2005, pp. 113–128.
- [11] X. Ou, W. F. Boyer, and M. A. McQueen, "A scalable approach to attack graph generation," in *Proceedings of the 13th ACM conference on Computer and communications security*, 2006, pp. 336–345.
- [12] D. Tayouri, N. Baum, A. Shabtai, and R. Puzis, "A survey of mulval extensions and their attack scenarios coverage," *IEEE Access*, 2023.
- [13] P. S. Patapanchala, C. Huo, R. B. Bobba, and E. Cotilla-Sanchez, "Exploring security metrics for electric grid infrastructures leveraging attack graphs," in *2016 IEEE Conference on Technologies for Sustainability (SusTech)*. IEEE, 2016, pp. 89–95.
- [14] S. Kriaa, L. Pietre-Cambacedes, M. Bouissou, and Y. Halgand, "A survey of approaches combining safety and security for industrial control systems," *Reliability engineering & system safety*, vol. 139, pp. 156–178, 2015.
- [15] S. Ceri, G. Gottlob, L. Tanca et al., "What you always wanted to know about datalog (and never dared to ask)," *IEEE transactions on knowledge and data engineering*, vol. 1, no. 1, pp. 146–166, 1989.
- [16] I. Semertzis, V. S. Rajkumar, A. Ştefanov, F. Franssen, and P. Palensky, "Quantitative risk assessment of cyber attacks on cyber-physical systems using attack graphs," in *2022 10th Workshop on Modelling and Simulation of Cyber-Physical Energy Systems (MSCPES)*. IEEE, 2022, pp. 1–6.
- [17] S. Hasan, A. Ghafouri, A. Dubey, G. Karsai, and X. Koutsoukos, "Vulnerability analysis of power systems based on cyber-attack and defense models," in *2018 IEEE Power & Energy Society Innovative Smart Grid Technologies Conference (ISGT)*. IEEE, 2018, pp. 1–5.
- [18] S. Hasan, A. Dubey, G. Karsai, and X. Koutsoukos, "A game-theoretic approach for power systems defense against dynamic cyber-attacks," *International Journal of Electrical Power & Energy Systems*, vol. 115, 2020. [Online]. Available: <http://www.sciencedirect.com/science/article/pii/S0142061519302807>
- [19] MITRE, "MITRE ATT&CK," URL: <https://attack.mitre.org>, 2021.
- [20] C. B. Browne, E. Powley, D. Whitehouse, S. M. Lucas, P. I. Cowling, P. Rohlfshagen, S. Tavener, D. Perez, S. Samothrakis, and S. Colton, "A survey of monte carlo tree search methods," *IEEE Transactions on Computational Intelligence and AI in Games*, vol. 4, no. 1, pp. 1–43, 2012.
- [21] M. Świechowski, K. Godlewski, B. Sawicki, and J. Mańdziuk, "Monte carlo tree search: A review of recent modifications and applications," *Artificial Intelligence Review*, vol. 56, no. 3, pp. 2497–2562, 2023.
- [22] S. Sahoo, T. Dragičević, and F. Blaabjerg, "Cyber security in control of grid-tied power electronic converters—challenges and vulnerabilities," *IEEE Trans. Emerg. Sel. Topics Power Electron.*, vol. 9, pp. 5326–5340, Oct. 2021.
- [23] C. Roberts, S.-T. Ngo, A. Milesi, S. Peisert, D. Arnold, S. Saha, A. Scaglione, N. Johnson, A. Kocheturov, and D. Fradkin, "Deep reinforcement learning for der cyber-attack mitigation," in *2020 IEEE International Conference on Communications, Control, and Computing Technologies for Smart Grids (SmartGridComm)*. IEEE, 2020, pp. 1–7.
- [24] W. Kersting, "Radial distribution test feeders," in *IEEE Power Engineering Society Winter Meeting*, 2001.
- [25] "Distribution automation feeder automation design guide," <https://www.cisco.com/c/en/us/td/docs/solutions/Verticals/Distributed-Automation/Feeder-Automation/DG/DA-FA-DG/DA-FA-DG.html>, accessed: [06/07/2023].
- [26] A. Liu, J. Chen, M. Yu, Y. Zhai, X. Zhou, and J. Liu, "Watch the unobserved: A simple approach to parallelizing monte carlo tree search," in *International Conference on Learning Representations*, 2020. [Online]. Available: <https://openreview.net/forum?id=BJlQJskDB>
- [27] A. Bhosekar and M. Ierapetritou, "Advances in surrogate based modeling, feasibility analysis, and optimization: A review," *Computers & Chemical Engineering*, vol. 108, pp. 250–267, 2018.